NANOSECOND TIME-RESOLVED EMISSION SPECTROSCOPY OF A FLUORESCENCE PROBE ADSORBED TO L-α-EGG LECITHIN VESICLES

J. HAMILTON EASTER, ROBERT P. DeTOMA, *and* LUDWIG BRAND

From the Biology Department and McCollum-Pratt Institute, The Johns Hopkins University, Baltimore, Maryland 21218

ABSTRACT Nanosecond time-resolved emission spectra (TRES) are fluorescence emission spectra obtained at discrete times during the fluorescence decay. The complete data-set obtainable is a surface representing the intensity at all wavelengths and times during the emission decay time. When 2-p-toluidinonaphthalene-6-sulfonate (2,6 p-TNS) is adsorbed to egg lecithin vesicles, an excited-state reaction associated with energetic changes of the emitting species occurs on the nanosecond time scale. Convolution of the fluorescence decay with the excitation response introduces an artifact in the time-dependent spectra. A procedure is described by which this artifact can be eliminated. The data for the generation of time-resolved emission spectra are obtained with a computer-interfaced instrument based on the single-photon counting method.

INTRODUCTION

Chromophores may undergo a variety of interactions with surrounding molecules in the time period between excitation and emission of light. This is due to the fact that the chemical and physical properties of excited molecules can be quite different from those in the ground state. These interactions frequently occur in the time period of a few tenths of a nanosecond to 50 or more nanoseconds, a time over which fluorescence decay measurements can be obtained.

The dramatic changes in fluorescence maxima and quantum yields often observed when fluorophores interact with proteins, nucleic acids, and membranes are reflections of exicted-state reactions. While these reactions can be observed with steady-state fluorescence measurements, their dynamics can be obtained directly by means of nanosecond fluorometry.

Nanosecond time-resolved emission spectra (TRES) are fluorescence emission spectra obtained at discrete times during the fluorescence decay. The complete data-set obtainable, $I(\lambda, t)$,[1] is a surface representing the intensity at all wavelengths and times during the fluorescence decay.

---

[1] $I(\lambda, t)$ or $I(\bar{\nu}, t)$ is the deconvolved intensity surface. $f(\lambda, t)$ or $f(\bar{\nu}, t)$ is the impulse response. $F(\lambda, t)$ is the convolved decay data and $F(\lambda)$ is the steady-state emission data.

In many instances the fluorescence emission energy does not change during the decay time. The kinetics of decay may be complex, but no further information is obtained by measuring the decay at various emission wavelengths. Numerous quenching reactions fall into this category. In other cases time-dependent spectral shifts are observed, but the data clearly indicate a mixture of two emitting species whose proportions change with time. Excited-state proton transfer as observed with β-naphthol (Loken et al., 1972) is an example of a two-state excited-state reaction. Fluorescence decay curves obtained at two appropriate wavelengths provide all the decay information required for kinetic analysis of a system of this type.

A more complex situation prevails for generalized excited-state solvation. In this case, a gradual shift of the fluorescence emission spectrum with time is observed and more than two emitting species appear to be involved. It is desirable to obtain data over the entire $I(\lambda, t)$ surface.

Ware et al. (1971), Chakrabarti and Ware (1971), and Egawa et al. (1971) have presented nanosecond time-resolved emission spectra of several dyes in viscous solvents. The results of these experiments fall into the category just mentioned. Brand and Gohlke (1971) have described similar results for 2-p-toluidinonaphthalene-6-sulfonate (2,6 p-TNS) dissolved in glycerol and adsorbed to serum albumin. Easter and Brand (1973) have shown that 2,6 p-TNS adsorbed to lecithin vesicles shows gradual nanosecond time-dependent red shifts of the fluorescence spectra. Thorndill (1973) has described similar red shifts with 2,6 p-TNS adsorbed to several native and denatured proteins.

There is thus ample evidence that solvent interactions on the nanosecond time scale occur with biochemical systems. The aim of the present paper is to show that quantitative measurements of these solvent interactions can be made on lipid bilayer systems. The distortion introduced by the convolution artifact can be eliminated by obtaining *deconvolved* nanosecond time-resolved emission spectra. Various ways of representing the kinetics of this system are discussed.

MATERIALS AND METHODS

L-α-egg lecithin was purified as previously reported (Easter and Brand, 1973). Lecithin vesicles were prepared by sonication under argon in a 0.01 M Tris-HCl, 0.1 M NaCl buffer at pH 8.5 as described by Huang (1969). Separation of the single bilayer vesicles was achieved on Sepharose 4B (Pharmacia) and vesicle concentration was determined by a modified lipid phosphorous analysis (Bartlett, 1959).

2,6 p-TNS was prepared by Seliskar (1971). Deionized water and laboratory reagent grade chemicals were used to make up all solutions.

The single-photon counting instrument used in this study is similar in principal to those previously described by Ware (1971), Schuyler and Isenberg (1971), Yguerabide (1972), and Loken (1973). Nanosecond time-resolved emission spectra are generated from decay curves obtained at various wavelengths throughout the emission band. In order to compensate for long-term timing drift or changes in shape of the lamp profile (Hazan et al., 1974), a semi-simultaneous collection of the lamp and the decay is carried out under fully automated computer control. The hardware interfacing between the computer and the various instrumental components is illustrated in Fig. 1. The computer can start and stop data accumulation of the
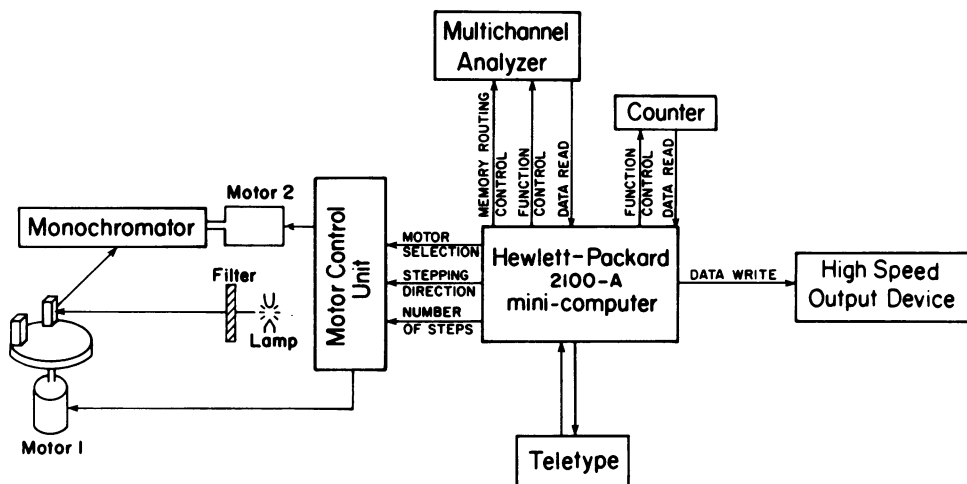
FIGURE 1 A Hewlett-Packard 2100A minicomputer with 16 K of core is interfaced to the single-photon counting fluorometer allowing versatile control of the instrumental conditions and data acquisition. The lamp is constructed as described by Yguerabide (1972) and is filled with 1 atm of N_2 or air. The electrodes, one of which is pointed and one round, are carefully aligned 0.4–0.45-mm apart. Power for the lamp, (7–7.5 kV), is provided by a 1150-1 Beckman high voltage power supply (Beckman Instruments, Inc., Fullerton, Calif.) The lamp is gated by a blocking oscillator thyratron circuit (Loken, 1973) at a constant repetition rate of 10,000 flashes/s. This provides a narrow lamp flash (2–2.5 ns at half intensity) with a stable intensity per flash and minimizes timing drifts of the lamp. The thyratron is mounted in a shielded and cooled housing attached to the lamp housing. The start pulse for the time to amplitude converter (TAC) is obtained from a high impedance antenna located 1–2 cm from the lamp and is passed through 100 ft of RG55/U cable (Lewis et al., 1973) giving about twofold attenuation of the signal before the discriminator input. The light is focused on the sample with a lens and is passed through an interference filter to select the desired exciting wavelength. For the data presented in this paper a 3300 Å Baird-Atomic band-pass filter (10-71-1) was used. The sample compartment contains two thermostated cuvette holders mounted on a horizontal turn-table. Either of the cuvettes can be positioned into the light path by rotation of the turntable. Emission from the sample cuvette can be observed simultaneously through a monochro-mator (Bausch & Lomb no. 33-86-45, Bausch & Lomb, Inc., Rochester, N.Y.) or by a monitor photomultiplier through a filter. The cuvette turntable and the emission monochromator are driven by Slo-Syn stepper-motors model HS-50L (200 steps per 360° revolution). The motors are controlled by Slo-Syn translators no. ST-1800BK (Superior Electric Co., Bristol, Conn.). The translators are activated by a signal from a Hewlett-Packard 16-bit relay output register (no. 12551B, Hewlett-Packard Co., Palo Alto, Calif.) installed in the computer. The computer, by means of the relay register, controls which motor is to be stepped, and the direction and the number of steps. A simple circuit allows either motor to be stepped forward or reversed inde-pendent of computer control. The detectors used are 56 DUVP/03 photomultipliers (Amperex Electronic Corp., Hicksville, N.Y.), which are operated at 2,500 V. The photomultiplier bases were obtained from Products for Research Inc., Danvers, Mass. (model PR-2200) and were modi-fied to provide for external control of the voltage levels on the grid and the first three dynodes. They are tuned for optimal sensitivity, output pulse shape, and homogeneous extraction field (Amperex Data Handbook, 1969). 100 ft of RG55/U cable is inserted between the photomulti-plier and the timing filter amplifier. The 5401B multichannel pulse height analyzer (MCA) and 5326B digital counter were obtained from Hewlett-Packard. The nuclear instrumentation bin, two 453 timing filter amplifiers, three 454 constant fraction timing discriminators, and a 437A TAC were obtained from Ortec, Inc., Oak Ridge, Tenn.

MCA and is capable of routing the lamp profile into one half of the MCA memory and the decay curve into the other half. It can start and stop the counter coincident with the MCA and can thus be used to keep a record of the counts from the monitor photomultiplier or total TAC starts (lamp flashes) so that the data can be corrected for photon pile-up if necessary (Coates, 1968).

The sequence of computer actions during the course of an experiment can be divided into three sections: collection, search, and output. In the collection phase the cuvette turntable is positioned with the fluorescence sample in the optical path, the monochromator is set to a specified wavelength, the MCA is directed to store in the first half of memory, the MCA is started in accumulation mode, and totalization with the counter is initiated. After a designated decay dwell time (typically 5-15 min) the MCA and the counter are stopped and the counter's data are transferred into the computer. The cuvette turntable is then positioned so that the scattering solution is in the optical path, the emission monochromator is set to the excitation wavelength, the MCA is directed to route into the second half of memory, and the MCA and counter are started in accumulation. After the specified lamp dwell time the MCA and the counter are stopped and the counter's data are transferred into the computer.

The computer now enters the second phase by searching the decay and lamp collections to determine whether the desired peak counts and/or total counts have been obtained. If the collection is not yet complete, a new set of dwell times are computed, based on the rates of collection, and the collection phase is repeated.

When the collection has reached the desired peak and/or total counts the computer enters the output phase. The lamp and decay curves are transferred to the high-speed output device along with their respective collection times, wavelengths, peak counts, total counts, counter monitor, and a curve-set index number. The computer then sets up for the next decay wavelength to be collected and repeats the entire procedure starting at the collection phase.

DATA ANALYSIS

The decay data $F(\lambda, t)$ obtained by means of the single-photon counting method are distorted since the desired impulse response $f(\lambda, t)$ is convolved with the exciting lamp flash $E(t)$ (Yguerabide, 1972). Convolved time-resolved emission spectra (TRES) obtained from these decay data are also distorted. For the generation of deconvolved TRES from complex decay curves it is desirable to recover $f(\lambda, t)$ empirically, i.e. without assuming a physical decay law for the system under study.

We have employed a nonlinear regression algorithm (Marquardt, 1963; Grinvald and Steinberg, 1974) for the deconvolution analysis of $F(\lambda, t)$. The fitting function that was chosen to model the experimental decay data is defined in terms of the convolution integral:

$$F(\lambda, t) = \int_0^t E(x - Q)\mu(x - Q)f(\lambda, t - x)\,dx, \qquad (1)$$

where $\mu(t)$ is the unit step function, Q is the energy-dependent time shift of the detector (Wahl et al., 1974; Gafni et al., 1975) which is determined independently with single lifetime reference dyes, and the impulse model is given by:

$$f(\lambda, t) = \sum_{j=1}^{P} \alpha_j e^{-t/\tau_j}. \qquad (2)$$

This choice of fitting function is completely general (Ware et al., 1973) since the regression search treats both α_j and τ_j as free parameters and p, the number of exponential terms, is arbitrary. It should be emphasized that the use of a sum of exponentials (Eq. 2) as the impulse model does not imply that the physical decay law at all wavelengths is a sum of exponentials. This is an empirical procedure for deconvolution and theoretical significance is not necessarily attached to the form of the model function or the values of the parameters derived from it.

The Marquardt algorithm of nonlinear least squares employs a dual search along the χ^2 hypersurface defined by:

$$\chi^2 = \sum_{i=1}^{N} \omega_i [F(\lambda, t) - F^{calc}(\lambda, t)]^2, \quad (3)$$

for the minimum value of χ^2. χ^2 is considered a function of the parameter increments that are defined with respect to initial parameter guesses (α_j^0, τ_j^0) which must be specified at the beginning of the search. The two searching paths (one for parameter guesses which establish χ^2 far removed from the minimum and the other for χ^2 values near the minimum) are portioned internally in the algorithm. ω_i is a statistical weighting factor defined by the principle of least squares and for the case of photon counting error may be approximated by:

$$\omega_i = 1/F(\lambda, t). \quad (4)$$

In order to judge the quality of recovery of $f(\lambda, t)$ from $F(\lambda, t)$, it is necessary to evaluate the "goodness of fit" of $F^{calc}(\lambda, t)$ with the experimental data $F(\lambda, t)$. Assuming that appropriate precautions (Lewis et al., 1973; Ware et al., 1973) have been taken to ensure the validity of Eq. 1, the approach to use in empirical deconvolution is to seek the best possible fit. With a large number of parameters and when the parameters are highly correlated, the final fit is somewhat dependent on the initial parameter guesses. For this reason we have found it essential to carry out these analyses in an interactive mode using the HP-2100 minicomputer interfaced with an oscilloscope display. The fit to the experimental data can be observed at any phase of the analysis and the search can be continued or reinitiated with new starting guesses if necessary. For the final criterion of "goodness of fit," we compare (a) values of the reduced χ^2 (Bevington, 1969); (b) residuals $= F^{calc}(\lambda, t) - F(\lambda, t)$; and (c) the autocorrelation function of the residuals (Grinvald and Steinberg, 1974).

Since both the α_j and τ_j are considered free parameters in this nonlinear method, typically only three or four exponential terms are necessary to obtain accurate deconvolutions. This has been verified for a variety of multi- and nonexponential decay data (both simulated and real). It has been found that nonlinear least squares with a multiexponential impulse model provides a powerful deconvolution method for fluorescence decay data obtained by the single-photon counting method.

Deconvolved TRES are generated directly from the impulse responses $f(\lambda, t)$ obtained as described above. The impulse responses are normalized to the steady-state
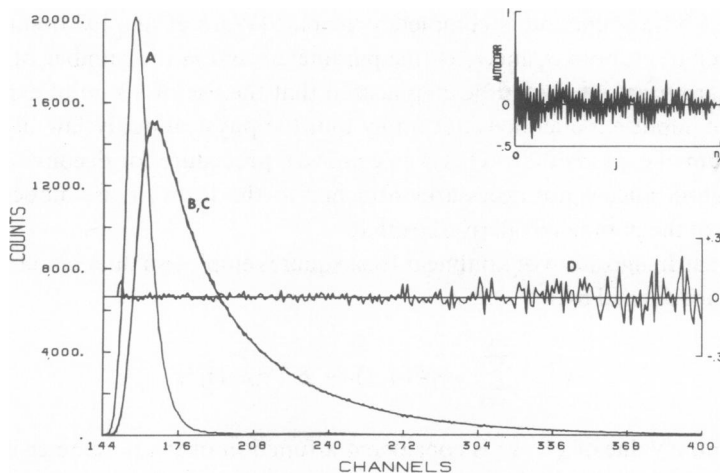
emission spectrum $F(\lambda)$ of the sample which is obtained under the same conditions of spectral bandwidth as $F(\lambda, t)$.[2] With $h(\lambda)$ defined by:

$$h(\lambda) = F(\lambda) \bigg/ \int_0^\infty f(\lambda, t) \, dt, \tag{5}$$

the properly normalized TRES is given by:

$$I(\lambda, t) = h(\lambda) f(\lambda, t). \tag{6}$$

$I(\lambda, t)$ may be converted to $I(\bar{\nu}, t)$ (wavenumber representation) and may be corrected for detector response at this time. The corrected TRES matrix is stored in the computer and may be displayed on the oscilloscope or on a digital plotter.

For the generation of convolved TRES the fluorescence decay data $F(\lambda, t)$ are

---

[2]Since the decay curves are collected for different periods of time, the impulse responses must be normalized either as described or to a constant excitation light flux intensity.
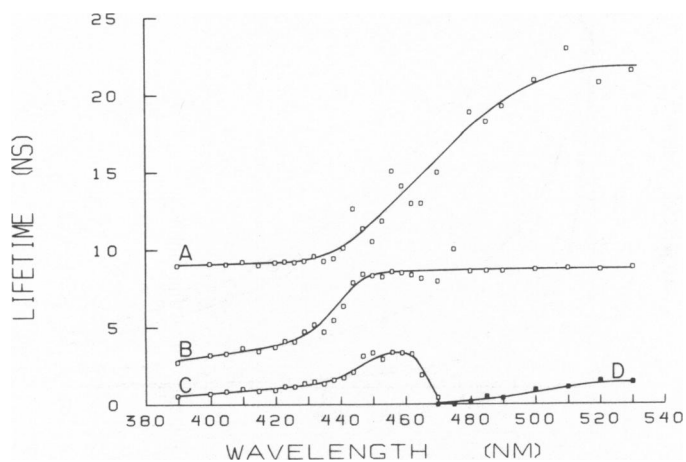
FIGURE 3 The decay times obtained by empirical deconvolution are shown as a function of wavelength, for 2,6 p-TNS adsorbed to L-α-egg lecithin vesicles at the conditions described in the legend to Fig. 2. Curves A–D connect the decay times of the exponential terms from the empirical deconvolution in order to help demonstrate their continuously varying nature. Open squares represent decay times having a positive pre-exponent and closed squares represent decay times having a negative pre-exponent.

normalized to constant lamp intensity as obtained from a monitor photomultiplier rather than to a steady-state spectrum.

RESULTS

The data presented here were obtained with 2,6 p-TNS adsorbed to single bilayer vesicles of egg lecithin. The results of a nonlinear least squares analysis of a decay curve obtained at 423 nm are shown in Fig. 2. Curve A is the lamp flash, curve B is the experimental decay curve, and curve C is the best fit to three exponential components obtained with the method of nonlinear least squares and convolved with the experimental lamp flash. Curve D represents the percent residuals between curves B and C. The autocorrelation of the residuals (Grinvald and Steinberg, 1974) is shown in the upper right and indicates the randomness of the residuals about zero.

The decay times obtained from the "empirical" deconvolution of 30 decay curves of 2,6 p-TNS adsorbed to lecithin vesicles over the wavelength range 390–530 nm are shown in Fig. 3. In this particular case an excellent fit to the decay at each wavelength was obtained with a maximum of three exponential terms. The decay times continuously vary over the entire wavelength region and the mean decay time increases with increasing wavelength. A short decay time with a negative pre-exponent, absent at the blue edge of the spectrum, appears at 470 nm and becomes more significant at the red end of the spectrum. No theoretical significance is necessarily attached to the numerical values of the exponential parameters other than to point out that the decay kinetics are complex and require several exponential terms to obtain a good fit, and that the short decay time with the negative amplitude demonstrates that a portion of the light
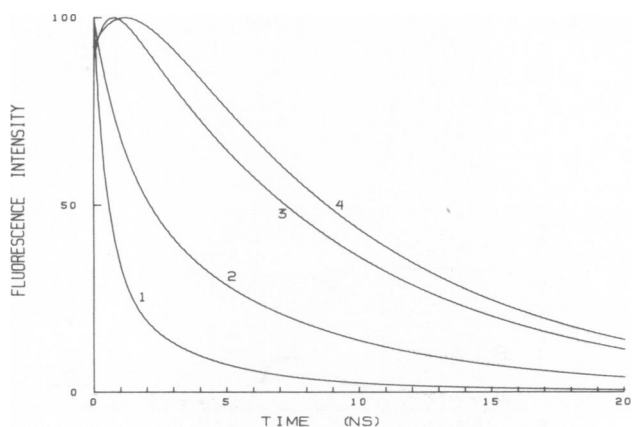
FIGURE 4 Peak normalized impulse responses generated from the deconvolution parameters of 2,6 p-TNS adsorbed to L-α-egg lecithin vesicles at the conditions described in the legend to Fig. 2. 1, 390 nm; 2, 423 nm; 3, 485 nm; 4, 530 nm.

observed at the red end of the spectrum is due to a reaction occurring in the excited state. These analyses are used to generate the impulse responses (deconvolved decay curves) shown in Fig. 4. Here the build-up of intensity at the red end of the spectrum is clearly evident. This figure also shows that the mean decay time of the dye's emission increases with increasing wavelength, a characteristic of excited-state solvation. Impulse responses of this type are used to generate the deconvolved time-resolved emission spectra shown in Fig. 5 for four representative time-windows. These spectra have been plotted as a function of energy and have been peak normalized for display pur-
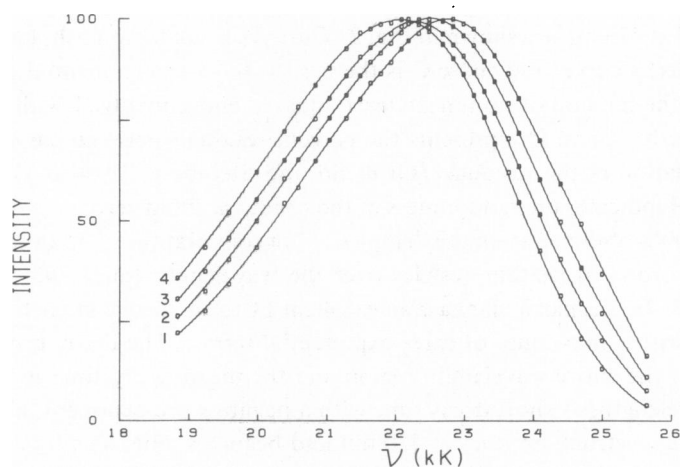

FIGURE 5 Peak normalized time-resolved emission spectra of 2,6 p-TNS adsorbed to L-α-egg lecithin vesicles at the conditions described in the legend to Fig. 2. 1, 1.02 ns; 2, 2.04 ns; 3, 4.08 ns; 4, 12.24 ns. Spectra are corrected for instrumental wavelength response. Kilokayser (kK) = 10^3 cm^{-1}.
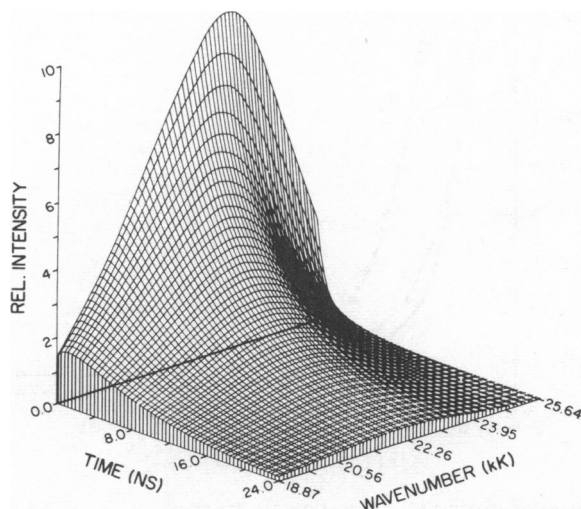
FIGURE 6 Three-dimensional representation of the fluorescence intensity as a function of both time and wavenumber for 2,6 p-TNS adsorbed to L-α-egg lecithin vesicles at the conditions described in the legend to Fig. 2.

poses. There is a clear time-dependent red shift while the spectral shape remains invariant with time. The complete interpolated data set of fluorescence intensity as a function of energy and time $I(\bar{\nu}, t)$ is shown in Fig. 6. Any line in this figure which is parallel to the $I(t)$ plane represents the decay kinetics at a particular energy and any line parallel to the $I(\bar{\nu})$ plane represents the emission spectrum at a particular time.

It was indicated above that failure to deconvolve leads to a distortion of the time-resolved emission spectra. This is illustrated by Fig. 7 which shows the peak maxima of the time-resolved emission spectra ($\bar{\nu}_{max}$) vs. time,[3] for both the convolved and the deconvolved data. The deconvolved $\bar{\nu}_{max}(t)$ is presented with its true time zero since it is generated from impulse responses. The convolved data, however, have no true time zero. Curves are shown with the initial rise of the lamp taken as time zero (solid squares) as suggested by Ware et al. (1971), and also with the peak of the lamp flash taken as time zero (open squares) as suggested by Easter and Brand (1973). Although the latter curve is closer to the deconvolved data, it is evident that the convolution introduces a distortion in both cases. It is necessary to use deconvolved time-resolved emission spectra if meaningful kinetic information is to be derived from such data.

The method of empirical deconvolution described above assumes that simple as well as complex decay kinetics can be fit accurately to a sum of exponentials by the method of nonlinear least squares. Using parameters similar to those obtained with the 2,6 p-TNS vesicle system, a simulation experiment was carried out to test this assumption,

---

[3] $\bar{\nu}_{max}$ is obtained by numerical differentiation based on local polynomial regression of the time-resolved emission spectra.
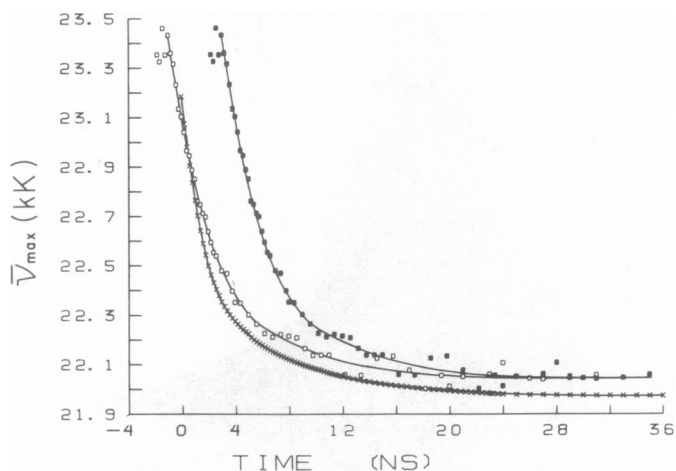
FIGURE 7   The emission maxima ($\bar{\nu}_{max}$) vs. time are presented for 2,6 *p*-TNS adsorbed to L-α-egg lecithin vesicles at the conditions described in the legend to Fig. 2.   X, deconvolved data; □, convolved data with peak of lamp flash (channel 160) taken as time zero; and ■, convolved data with initial rise of lamp flash (channel 140) taken as time zero.   Channel number reference for the lamp profile can be seen in Fig. 2.

to verify the distortion introduced by convolution, and to evaluate the software used to generate the time-resolved emission spectra.

A time-resolved emission spectrum at time-zero was defined as a Gaussian curve with a bandwidth of 4.4 kiloKaysers (kK).   The bandwidth was set constant with time and the peak position was shifted to the red at a rate defined by a double exponential with decay times of 1.4 and 7.8 ns in the proportions of 1 to 1.9.   The intensity of the spectra was damped according to a double exponential decay law with decay times of 1.57 and 8.4 nsec in the proportions of 1 to 3.3.

A set of numerical impulse responses (deconvolved decay curves) was generated from the time-resolved emission spectra stimulated as described above.   The kinetics of the impulse responses are complex and nonexponential (this is shown theoretically elsewhere).[4] Each impulse response was convolved with an experimental lamp flash to yield a set of convolved decay curves.

The simulated decay curves obtained as described above were used to generate a set of convolved and deconvolved time-resolved emission spectra.   Fig. 8 shows $\bar{\nu}_{max}(t)$ for both convolved and deconvolved spectra.   The deconvolved curve was superimposable with the model function for $\bar{\nu}_{max}(t)$, thus showing the validity of the deconvolution procedure.   Furthermore, the convolved $\bar{\nu}_{max}(t)$ curve shows the same distortion that is observed in the experimental data shown in Fig. 7.   The identity between the original time-dependent spectra and those obtained after convolution of the decay curves followed by deconvolution with the method of nonlinear least squares serves as a verification of the data analysis procedure.

---

[4] DeToma, R. P., J. H. Easter, and L. Brand. 1976. *J. Am. Chem. Soc.* In press.
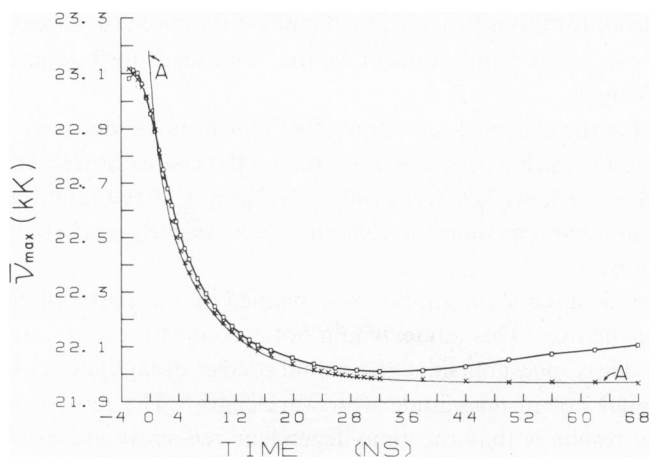
FIGURE 8 Results of simulated TRES showing $\bar{\nu}_{max}(t)$. The solid line A represents the model used in the simulation; □, the convolved results using an experimental lamp flash where its peak, channel 160, was taken as time-zero; X, the convolved results using a simulated Gaussian lamp flash which existed only between channels 140 and 180 where its peak, channel 160, was taken as time zero.

The positive deviation of $\bar{\nu}_{max}$ at long times which is present in the experimental convolved data (Fig. 7) and the simulation using a real lamp (Fig. 8) is absent if a Gaussian lamp flash which is truly dead at early times is used in the simulation (Fig. 8). Thus it should be emphasized that convolution influences the results not only at early times where the lack of a true time zero is self-evident, but also at late times, particularly when the intensity of the decay has decreased two or three orders of magnitude.

DISCUSSION

Since excited chromophores have characteristics different from those of their ground-state counterparts, they may relax to a new equilibrium with surrounding molecules. The nature of any excited-state process will depend on the character of the excited chromophore and that of the surrounding molecules. The ability to detect excited-state reactions by means of time-resolved fluorescence spectroscopy depends on the kinetic factor. To be observable the reactions must occur within the time-window defined by the resolution of the instrument on the one hand and the excited-state lifetime on the other.

It has been shown here that the fluorescence emission spectra of 2,6 p-TNS adsorbed to egg lecithin bilayer vesicles exhibit red-shifts on the nanosecond time-scale. Although the time-resolved emission spectra obtained directly are distorted by convolution error, this difficulty is readily eliminated by an empirical deconvolution procedure. Time-dependent red-shifts quite similar to those described here with vesicles are observed with 2,6 p-TNS dissolved in glycerol[4] but not when the dye is dissolved in a nonviscous liquid solution.

The time-dependent red-shifts described here are clearly associated with excited-state

processes. Evidence for this is provided by the negative amplitude associated with one of the decay times at the red end of the emission. This leads to the rise of the impulse response at early times.

It is unlikely that the observed time-dependent red-shifts are due only to a two-state excited-state reaction such as exciplex formation. Reversible or irreversible two-state reactions would give rise to two decay times invariant in magnitude but changing in relative proportion with emission wavelength. This is clearly not what has been observed in this study.

The time-dependent red-shifts cannot be explained by the existence of two different binding sites for the dye. This model would not account for the negative amplitudes observed in the decay measurements and would predict decay times changing in relative proportion but not in magnitude with wavelength. The most reasonable interpretation of the results is that the time-dependent red-shifts are associated with a general relaxation of polar residues about the excited chromophore on the nanosecond time scale. This implies not only that the probe is surrounded by polar residues but that these groups have restricted motion as compared to that expected in a liquid solution. An alternative explanation for the results is that the binding constant for the probe decreases in the excited state and that the red-shift is associated with dye molecules on their way off the vesicles. It is suggested that a study of the nanosecond time-resolved spectral characteristics of probes in relation to membrane structure and function will be of interest.

REFERENCES

AMPEREX DATA HANDBOOK. 1969. Amperex Electronic Corp., New York. 6.

BARTLETT, G. R. 1959. Phosphorus assay in column chromatography. *J. Biol. Chem.* **234**:466.

BEVINGTON, P. R. 1969. Data Reduction and Error Analysis for the Physical Sciences. McGraw Hill Book Company, Inc., New York.

BRAND, L., and J. R. Gohlke. 1971. Nanosecond time-resolved fluorescence spectra of a protein-dye complex. *J. Biol. Chem.* **246**:2317.

CHAKRABARTI, S. K., and W. R. WARE. 1971. Nanosecond time-resolved emission spectroscopy of 1-anilino-8-naphthalene sulfonate. *J. Chem. Phys.* **55**:5494.

COATES, P. B. 1968. The correction for photon "pile-up" in the measurement of radiative lifetimes. *J. Sci. Instrum. (J. Physics E).* **1**:878.

EASTER, J. H., and L. BRAND. 1973. Nanosecond time-resolved emission spectroscopy of a fluorescence probe bound to L-α-egg lecithin vesicles. *Biochem. Biophys. Res. Commun.* **52**:1086.

EGAWA, K., N. NAKASHIMA, N. MATAGA, and C. YAMANAKA. 1971. Time-resolved fluorescence studies on charge transfer interactions in 1,2,4,5-tetracyanobenzene-toluene complex. *Bull. Chem. Soc. Japan.* **44**:3287.

GAFNI, A., R. L. MODLIN, and L. BRAND. 1975. Analysis of fluorescence decay curves by means of the laplace transformation. *Biophys. J.* **15**:263.

GRINVALD, A., and I. Z. STEINBERG. 1974. On the analysis of fluorescence decay kinetics by the method of least squares. *Anal. Biochem.* **59**:583.

HAZAN, G., A. GRINVALD, M. MYTAL, and I. Z. STEINBERG. 1974. An improvement of nanosecond fluorimeter to overcome drift problems. *Rev. Sci. Instrum.* **45**:1602.

HUANG, C. 1969. Studies on phosphatidyl-choline vesicles. Formation and physical characteristics. *Biochemistry.* **8**:344.

LEWIS, C., W. WARE, L. DOEMENY, and T. NEMZEK. 1973. The measurement of short-lived fluorescence decay using the single photon counting method. *Rev. Sci. Instrum.* **44**:107.

LOKEN, M. R. 1973. Determination of rates of excited-state reactions using nanosecond fluorometric techniques. Ph.D. dissertation. The Johns Hopkins University, Baltimore, Md.

LOKEN, M. R., J. W. HAYES, J. R. GOHLKE, and L. BRAND. 1972. Excited-state proton transfer as a biological probe. Determination of rate constants by means of nanosecond fluorometry. *Biochemistry.* **11**:4779.

MARQUARDT, D. W. 1963. An algorithm for least-squares estimation of non-linear parameters. *J. Soc. Ind. Appl. Math.* **11**:431.

SCHUYLER, R., and I. Isenberg. 1971. A monophoton fluorometer with energy discrimination. *Rev. Sci. Instrum.* **42**:813.

SELISKAR, C. J., and L. BRAND. 1971. Electronic spectra of 2-amino-naphthalene-6-sulfonate and related molecules. I. General properties and excited-state reactions. *J. Am. Chem. Soc.* **93**:5405.

THORNDILL, D. T. 1973. Solvent relaxation about 2-p-toluidinonaphthalene-6-sulfonate in solution and adsorbed to proteins. Ph.D. dissertation. The Johns Hopkins University, Baltimore, Md.

WAHL, P., J. C. AUCHET, and B. DONZEL. 1974. The wavelength dependence of the response of a pulse fluorometer using the single photoelectron counting method. *Rev. Sci. Instrum.* **45**:28.

WARE, W. R. 1971. Transient luminescence measurements. *In* Creation and Detection of the Excited State. A. A. Lamola, editor. *IA:* Marcel Dekker, Inc., New York. 213.

WARE, W. R., L. J. DOEMENY, and T. L. NEMZEK. 1973. Deconvolution of fluorescence and phosphorescence decay curves. A least squares method. *J. Phys. Chem.* **77**:2038.

WARE, W. R., S. K. LEE, G. J. BRANT, and P. P. CHOW. 1971. Nanosecond time-resolved emission spectroscopy: spectral shifts due to solvent-excited solute relaxation. *J. Chem. Phys.* **54**:4729.

YGUERABIDE, J. 1972. Nanosecond fluorescence spectroscopy of macromolecules. *In* Methods in Enzymology. Academic Press, Inc., New York.